Comparisons of Channel Estimation for OFDM-based and Wavelet-based Underwater Acoustic Communications

Chenhao Qi*† and Lenan Wu†
*Key Laboratory of Underwater Acoustic Signal Processing of Ministry of Education, China
†School of Information Science and Engineering, Southeast University, Nanjing 210096, China
Email: qch@seu.edu.cn

***Abstract*—In this paper, a wavelet-based underwater acoustic (UWA) communication system is proposed. The convolutional structure of the UWA channel is exploited and the pilot assisted channel estimation is formulated as a sparse recovery problem. Then the restricted isometry property (RIP) of the measurement matrix is investigated via eigenvalue analysis and Gersgorin circle theorem. It's proved that the sparse recovery of the wavelet-based UWA channel satisfies the RIP. With the above setup, comparisons of channel estimation for OFDM-based and wavelet-based UWA communication systems are deployed. Simulation results show that the wavelet-based system achieves more accurate channel estimation performance than the OFDM-based system under the same conditions of bandwidth, duration, data rate and channel profile.**

***Index Terms*—Underwater acoustic (UWA) communications, sparse channel estimation, compressed sensing (CS), wavelet, OFDM.**

I. Introduction

With the increasing interest in underwater acoustic (UWA) communications, the study of high rate and reliable digital communications for submarines and various underwater vehicles is receiving a great deal of attention and promoting applications such as deep sea fishing, oil exploration, wildlife tracking and environmental monitoring. However, three main challenges exist in the development of UWA communications. The first one is the scarce frequency resource. UWA signals experience considerable attenuation at high frequency range due to the fact that the water absorption grows rapidly as the distance and the carrier frequency increase. On the other hand, UWA signal at low frequency is severely contaminated by the UWA channel noise. Therefore the valid band for UWA communications is only available at medium frequency and is very limited. For example, to communicate at the distance of 100 kilometers, only 1 kHz bandwidth is available. The second challenge is the Doppler effect. Since the bandwidth is comparable to the carrier frequency in UWA communications, it's a typical wideband system where the Doppler shift cannot be regarded as the same for the whole band. Moreover, considering that the speed of sound, i.e., 1500 m/s in the seawater, is very slow compared to the speed of electro-magnetic waves in the air, any relative motion between the transmitter and the receiver will cause severe Doppler distortion. The last challenge is the abundant multipath propagation. In addition to the direct path, the acoustic signal propagates via multiple reflections from the surface, bottom and other objects. The large delay spread leads to strong frequency selectivity that may be highly time-varying. The inter-symbol interference (ISI) may spread over several hundreds of symbol periods, which can bring heavy burden to the front-end preprocessing for combatting the channel effect at the receiver.

Recently, orthogonal frequency-division multiplexing (OFDM) which has prevailed in terrestrial wireless systems has also been applied to UWA communications [1], [2]. OFDM transforms the frequency-selective channel into several parallel flat-fading narrowband subchannels, where each subband only needs a single-tap equalizer. Therefore, the high complexity associated with the long decision-feedback equalizer (DFE) in single carrier systems is mitigated. More recently, the wavelet has been applied for UWA communications due to its inherent advantage to filter out narrow band interference by wavelet denoising [3], [4]. In OFDM, it usually requires a guard interval, e.g., cyclic prefix (CP) or zero padding (ZP), to combat inter-channel interference (ICI) and ISI caused by channel multipaths. The overhead of the guard interval is saved in wavelet systems, especially for UWA channel whose delay spread is usually very large. Additionally, OFDM employs rectangular or other types of window to suppress side lopes of power spectrum, which produces ICI and ISI that damage the orthogonality of subcarriers. It's demonstrated in [5] that lower ICI and ISI than OFDM can be achieved in wavelet systems. In particular, a wavelet filter bank system can be regarded as the extension of an OFDM system where the Fourier basis is employed instead of the wavelet basis [6].

Nevertheless, one of the largest barriers blocking UWA communications is the UWA channel distortion. Compared to single carrier systems, OFDM estimates the channel before making the one-tap channel equalization, which substantially reduces the receiver's complexity. And further combining the recently emerged compressed sensing (CS) techniques, UWA channel estimation is much more simplified. The channel impulse response (CIR) can be reconstructed through sparse recovery algorithms since the UWA channel is usually dominated by a small number of significant paths, resulting in a sufficient sparse CIR. This topic is currently undergoing explo-

978-1-4673-5939-9/13/$31.00 ©2013 IEEE

sive discussions [2], [7], [8]. Many CS algorithms including matching pursuit (MP), orthogonal matching pursuit (OMP) and basis pursuit (BP) have been applied for UWA OFDM channel estimation [9].

In this paper, we first construct a wavelet-based UWA communication system. We exploit the convolutional structure and formulate the pilot assisted UWA channel estimation as a sparse recovery problem. Then we investigate the restricted isometry property (RIP) of the measurement matrix via eigenvalue analysis and Gersgorin circle theorem. With these preparations, we compare the channel estimation performance for the wavelet-based and OFDM-based UWA communication systems under the same conditions of bandwidth, duration, channel profile and data rate.

The notation used in this paper is according to the convention. Symbols for matrices (upper case) and vectors (lower case) are in boldface. $(\cdot)^{\mathrm{T}}$, $|\cdot|$, $\|\cdot\|_2$, $\lfloor\cdot\rfloor$, $\mathbb{R}$, $diag\{\cdot\}$, $\boldsymbol{I}_L$ and $\mathcal{CN}$ denote transpose, absolute value, ℓ_2-norm, the floor, the set of real number, the diagonal matrix, the identity matrix with dimension L and the complex Gaussian distribution, respectively.

II. Problem Formulation

We consider the UWA channel that has a time-varying multipath CIR as

$$h(\tau,t)=\sum_{i=1}^{S}\xi_i(t)\delta(\tau-\tau_i(t)) \tag{1}$$

where S, $\xi_i(t)$ and $\tau_i(t)$ are the number of total path, the path attenuation and path delay of the ith time-varying path, respectively. We adopt two assumptions as follows.

1) All paths have the same Doppler scaling factor $\alpha(t)$ such that

$$\tau_i(t)\approx\tau_i-\alpha(t)t \tag{2}$$

which supposes the dominant Doppler shift is caused by the relative movement between the transmitter and the receiver [1].

2) $\xi_i(t)$, $\tau_i(t)$ and $\alpha(t)$ are constant over each data block which contains data symbols and training symbols. This assumption is reasonable because the UWA channel coherence time is usually on the order of seconds while the duration of each data block is no more than hundreds of milliseconds. In fact this assumption is common when we deal with time-varying channels.

With these two assumptions, we directly sample the received passband signal without down conversion since the frequency range used for UWA communications is usually in tens of thousands of hertz, which is more convenient to implement in software-defined radio (SDR). In order to estimate the resampling factor, we design each data block containing one preamble and one postamble. In [10], a structure of preamble is proposed where it consists of two identical OFDM symbols and one CP. And correspondingly, a bank of self-correlators is employed for the receiver with each of the self-correlators matched to a different duration. However, the shortcoming of this approach is that the estimation accuracy relies on the number of self-correlators. Therefore in this paper, we design the preamble and postamble to be linear-frequency-modulated (LFM) signals. By cross-correlating the received signal with the known preamble and postamble, the receiver estimates the length of each data block and figures out the resampling factor, which is more flexible than using a bank of self-correlators. After resampling, there is only a residual carrier frequency offset (CFO) which can be viewed as uniform for the whole bandwidth. Hence, a wideband system is converted into a narrow band system with frequency-independent CFO, which can be conveniently compensated in the wavelet filter bank systems [11].

According to the filter bank theories in wavelet, the scaling function and the wavelet function can be considered as a low pass filter and a high pass filter, respectively. Figure 1 gives a block diagram of wavelet-based UWA communication system. The serial data stream $x(n)$ is first converted into M parallel multirate data streams, $x_0(n)$, $x_1(n)$, …, $x_{M-1}(n)$, where

$$x_i(n)=\begin{cases}x(2^{i+1}\cdot n-2^i), & i=0,1,\ldots,M-2\\ x(2^{M-1}\cdot n-2^{M-1}). & i=M-1\end{cases} \tag{3}$$

Then they pass through a bank of reconstruction wavelet filters with each filter comprising an upsampling operation $\uparrow n_i$ $(i=0,1,\ldots,M-1)$ and a filtering operation $f_i(n)$ $(i=0,1,\ldots,M-1)$. The output of every branch is combined together, denoted as $s(n)$. Then $s(n)$ is sent into the UWA channel. At the receiver, $r(n)$ is first input into a bank of decomposition wavelet filters with each filter comprising a digital filtering operation $g_i(n)$ $(i=0,1,\ldots,M-1)$ and a downsampling operation $\downarrow n_i$ $(i=0,1,\ldots,M-1)$. After that, the parallel data streams are converted into a serial data stream $y(n)$.

For a Haar wavelet, the scaling function and the wavelet function can be written as

$$p(n)=\frac{1}{\sqrt{2}}\delta(n)+\frac{1}{\sqrt{2}}\delta(n-1) \tag{4}$$

$$q(n)=\frac{1}{\sqrt{2}}\delta(n)-\frac{1}{\sqrt{2}}\delta(n-1) \tag{5}$$

respectively. After the cascaded filter conversion and the Z-transform, we have

$$n_i=\begin{cases}2^{i+1}, & i=0,1,\ldots,M-2\\ 2^{M-1}, & i=M-1\end{cases} \tag{6}$$

and

$$f_i(z)=\begin{cases}\prod_{k=0}^{M-1}p(z^{2^k}), & i=M-1\\ q(z^{2^i})\prod_{k=0}^{i-1}p(z^{2^k}), & i=1,\ldots,M-2\\ q(z), & i=0\end{cases} \tag{7}$$

where $f_i(z)$ is the Z-transform of $f_i(n)$, denoted as

$$f_i(z)=\sum_{n=-\infty}^{+\infty}f_i(n)z^{-n}. \tag{8}$$

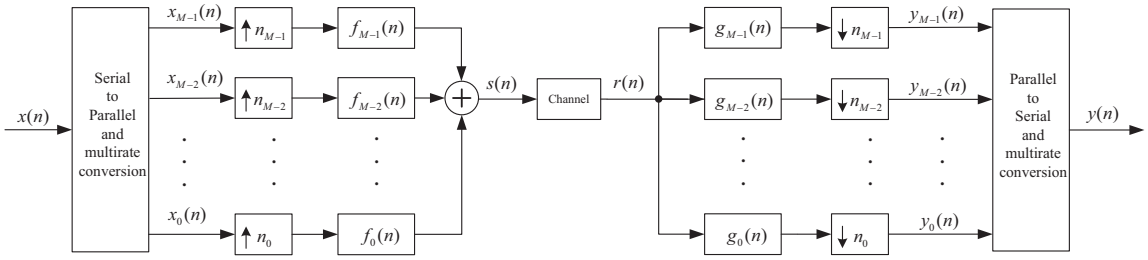

Fig. 1. Wavelet-based UWA communication system.

Therefore we obtain

$$\begin{aligned} s(n) &= \sum_{i=0}^{M-1}\sum_{k=0}^{\infty} x_i(k) f_i(n-2^{i+1}k) \\ &= \sum_{k=0}^{\infty}\Big[x(2^{M-1}\cdot k - 2^{M-1}) \\ &\quad + \sum_{i=0}^{M-2} x(2^{i+1}\cdot k - 2^i)\Big] f_i(n-2^{i+1}k). \end{aligned} \tag{9}$$

Now we can formulate the received signal $r(n)$ as the discrete time convolution between $s(n)$ and $h(n)$, which is denoted as

$$r(n) = s(n) * h(n) + \eta(n) \tag{10}$$

where $\eta(n)$ is the sample of additive white Gaussian noise (AWGN). Let L denote the length of $h(n)$ and suppose the training sequence to be $\{s(n), n = 0, 1, \ldots, N_T - 1\}$ ($N_T > L$). The resulting input-output relation of (10) can be represented as a matrix-vector product

$$\tilde{\boldsymbol{r}} = \tilde{\boldsymbol{A}}\boldsymbol{h} + \tilde{\boldsymbol{\eta}} \tag{11}$$

where $\tilde{\boldsymbol{r}} = [r(0), r(1), \cdots, r(N_T - 1)]^{\mathrm{T}}$ and $\boldsymbol{h} = [h(0), h(1), \cdots, h(L-1)]^{\mathrm{T}}$. $\tilde{\boldsymbol{\eta}} = [\eta(0), \eta(1), \cdots, \eta(N_T - 1)]^{\mathrm{T}} \sim \mathcal{CN}(\boldsymbol{0}, \sigma_\eta^2 \boldsymbol{I}_{N_T})$ is a noise vector with each component to be an AWGN sample. And

$$\tilde{\boldsymbol{A}} = \begin{bmatrix} s(0) & s(-1) & \cdots & s(-L+1) \\ s(1) & s(0) & \cdots & s(-L+2) \\ \vdots & \vdots & \ddots & \vdots \\ s(N_T-1) & s(N_T-2) & \cdots & s(N_T-L) \end{bmatrix} \tag{12}$$

contains the known training sequences $\{s(n), n = 0, 1, \ldots, N_T - 1\}$ as well as the unknown sequences $\{s(n), n = -L+1, -L+2, \ldots, -1\}$ that locate in the upper-right triangular area of $\tilde{\boldsymbol{A}}$. The unknown sequences include data symbols and null symbols that are unknown to the receiver. Therefore, we cannot directly use $\tilde{\boldsymbol{A}}$ for channel estimation. Instead, we have to use a submatrix as

$$\boldsymbol{A} = \begin{bmatrix} s(L-1) & s(L-2) & \cdots & s(0) \\ s(L) & s(L-1) & \cdots & s(1) \\ \vdots & \vdots & \ddots & \vdots \\ s(N_T-1) & s(N_T-2) & \cdots & s(N_T-L) \end{bmatrix} \tag{13}$$

of $\tilde{\boldsymbol{A}}$ for channel estimation. We observe that all components of $\boldsymbol{A}$ are the known training symbols from $\{s(n), n = 0, 1, \ldots, N_T - 1\}$. The dimension of $\tilde{\boldsymbol{A}}$ and $\boldsymbol{A}$ are N_T by L and $(N_T - L + 1)$ by L, respectively. Then (11) is reformulated as

$$\boldsymbol{r} = \boldsymbol{A}\boldsymbol{h} + \boldsymbol{\eta} \tag{14}$$

where $\boldsymbol{r} = [r(L-1), r(L), \ldots, r(N_T - 1)]^{\mathrm{T}}$ and $\boldsymbol{\eta} = [\eta(L-1), \eta(L), \ldots, \eta(N_T - 1)]^{\mathrm{T}}$. If $N_T \geq 2L - 1$, (14) is an over-determined problem and the least squares (LS) can be applied. However, we are more interested in the under-determined case where $L \leq N_T < 2L - 1$ and the rows of $\boldsymbol{A}$ are less than its columns. In this case, only a small number of training sequence is required, which indicates the improvement in data rate and spectrum efficiency. Combining with the recently emerged CS techniques, (14) is undergoing extensive discussions on the sparse recovery performance of $\boldsymbol{h}$ from the observations $\boldsymbol{r}$ and the measurement matrix $\boldsymbol{A}$. So in the following section, we investigate the RIP of $\boldsymbol{A}$.

III. Restricted Isometry Property

Recent advances in CS show that $\boldsymbol{h}$ in (14) can be recovered from $\boldsymbol{r}$ with high accuracy when $\boldsymbol{A}$ satisfies RIP [12].

Definition: $\boldsymbol{A} \in \mathbb{R}^{m \times n}$ satisfies RIP if

$$(1-\delta)\|\boldsymbol{h}\|_2^2 \leq \|\boldsymbol{A}\boldsymbol{h}\|_2^2 \leq (1+\delta)\|\boldsymbol{h}\|_2^2 \tag{15}$$

holds for all S-sparse vectors $\boldsymbol{h} \in \mathbb{R}^n$ ($\|\boldsymbol{h}\|_0 \leq S$).

It can be easily obtained from (15) that

$$\begin{aligned} &(1-\delta)\|\boldsymbol{h}\|_2^2 \leq \lambda_{\min}\|\boldsymbol{h}\|_2^2 \\ &\quad \leq \|\boldsymbol{A}\boldsymbol{h}\|_2^2 \leq \lambda_{\max}\|\boldsymbol{h}\|_2^2 \leq (1+\delta)\|\boldsymbol{h}\|_2^2 \end{aligned} \tag{16}$$

where $\lambda_{\min}$ and $\lambda_{\max}$ denote the minimum and maximum eigenvalues of $\boldsymbol{A}^{\mathrm{T}}\boldsymbol{A}$, respectively. Then this sufficient condition for RIP is simplified as

$$1 - \delta \leq \lambda_{\min} \leq \lambda_{\max} \leq 1 + \delta \tag{17}$$

Here we start with the discussion on the RIP condition of $\boldsymbol{A}$ in (14) before applying CS algorithms for the wavelet-based UWA communication system. The toeplitz compressed sensing matrices have been studied in [13]. However, here we treat it in a simplified approach. First we normalize $\boldsymbol{A}$ so that each column of $\boldsymbol{A}$ is normalized to be one. We have

$$\boldsymbol{A} = \boldsymbol{X}\boldsymbol{D} \tag{18}$$

where $\boldsymbol{D} = diag\{\kappa_1, \kappa_2, \ldots, \kappa_L\}$ is a diagonal matrix with each diagonal component to be a normalized coefficient and

$$\boldsymbol{X} = \begin{bmatrix} \frac{s(L-1)}{\kappa_1} & \frac{s(L-2)}{\kappa_2} & \cdots & \frac{s(0)}{\kappa_L} \\ \frac{s(L)}{\kappa_1} & \frac{s(L-1)}{\kappa_2} & \cdots & \frac{s(1)}{\kappa_L} \\ \vdots & \vdots & \ddots & \vdots \\ \frac{s(N_T-1)}{\kappa_1} & \frac{s(N_T-2)}{\kappa_2} & \cdots & \frac{s(N_T-L)}{\kappa_L} \end{bmatrix} \tag{19}$$

is an ℓ_2-normalized matrix. $\boldsymbol{X} \in \mathbb{R}^{N\times L}$ where $N = N_T - L + 1$. In this way we guarantee that every diagonal component of $\boldsymbol{V} = \boldsymbol{X}^{\mathrm{T}}\boldsymbol{X}$ is one. Let $\boldsymbol{V}_{i,j}$ represent the component in i-th row, j-th column of $\boldsymbol{V}$. We have $\Big\{\boldsymbol{V}_{i,i} = 1 \;\Big|\; i \in \{1, 2, , \ldots, L\}\Big\}$.

Suppose $\tilde{\boldsymbol{h}} = \boldsymbol{D}\boldsymbol{h}$. We reformulate (14) as

$$\boldsymbol{r} = \boldsymbol{X}\tilde{\boldsymbol{h}} + \boldsymbol{\eta}. \tag{20}$$

After $\tilde{\boldsymbol{h}}$ is reconstructed, we can obtain $\boldsymbol{h}$ by

$$\boldsymbol{h} = \boldsymbol{D}^{-1}\tilde{\boldsymbol{h}}. \tag{21}$$

It's observed that each off-diagonal component of $\boldsymbol{V}$ is the inner product between two different columns of $\boldsymbol{X}$, i.e.,

$$\begin{aligned} \boldsymbol{V}_{1,2} \;=\; & \Big(s(L-2)s(L-1) + s(L-1)s(L) \\ & + s(L)s(L+1) + s(L+1)s(L+2) \\ & + \cdots + s(N_T-3)s(N_T-2) \\ & + s(N_T-2)s(N_T-1)\Big) \Big/ \kappa_1\kappa_2. \end{aligned} \tag{22}$$

It's possible to split the summation into two groups as

$$\begin{aligned} \boldsymbol{V}_{1,2} \;=\; & \Big(s(L-2)s(L-1) + s(L)s(L+1) + \cdots \\ & + s(N_T-3)s(N_T-2)\Big) \Big/ \kappa_1\kappa_2 \\ & + \Big(s(L-1)s(L) + s(L+1)s(L+2) \\ & + \cdots + s(N_T-2)s(N_T-1)\Big) \Big/ \kappa_1\kappa_2 \end{aligned} \tag{23}$$

so that the items of the summation within each group are independent. We denote

$$\begin{aligned} \boldsymbol{V}^{(1)}_{1,2} \;=\; & s(L-2)s(L-1) + s(L)s(L+1) + \cdots \\ & + s(N_T-3)s(N_T-2) \end{aligned} \tag{24}$$

and

$$\begin{aligned} \boldsymbol{V}^{(2)}_{1,2} \;=\; & s(L-1)s(L) + s(L+1)s(L+2) + \cdots \\ & + s(N_T-2)s(N_T-1). \end{aligned} \tag{25}$$

Then

$$\boldsymbol{V}_{1,2} = \Big(\; \boldsymbol{V}^{(1)}_{1,2} + \boldsymbol{V}^{(2)}_{1,2} \;\Big) \Big/ \kappa_1\kappa_2. \tag{26}$$

Considering traditional modulation schemes such as phase shift keying (PSK) and quadrature amplitude modulation (QAM), the constellation points are symmetrically distributed and thus the mean of these items is zero. Also notice that the amplitude of these points is finite because they usually lie within a circular or a rectangular area. Then we have $\mathbb{E}\Big\{s(n)\Big\} = 0$ and

$$\Big|s(n)\Big| \le \kappa, \;\; n = 0, 1, \ldots, N_T. \tag{27}$$

According to the Hoeffding's inequality which states

$$\Pr\left(\Big|\sum_{i=1}^{k}\omega_i - \mathbb{E}\Big\{\sum_{i=1}^{k}\omega_i\Big\}\Big| \ge t\right) \le 2\exp\Big(-\frac{2t^2}{\sum_{i=1}^{k}(b_i-a_i)^2}\Big) \tag{28}$$

where

$$\Big\{\; \omega_i \mid \omega_i \in [a_i, b_i], i \in \{1, 2, \ldots, k\} \;\Big\} \tag{29}$$

are independent bounded random variables, we get

$$\Pr\Big(\boldsymbol{V}^{(1)}_{1,2} \ge t\Big) \le 2\exp\Big(-\frac{t^2}{(N_T-L+1)\kappa^4}\Big) \tag{30}$$

and

$$\Pr\Big(\boldsymbol{V}^{(2)}_{1,2} \ge t\Big) \le 2\exp\Big(-\frac{t^2}{(N_T-L+1)\kappa^4}\Big). \tag{31}$$

Therefore we get

$$\begin{aligned} & \Pr\Big(\;\Big|\boldsymbol{V}_{1,2}\Big| \ge \frac{\delta}{L-1}\Big) \\ & \le \Pr\Big(\Big|\boldsymbol{V}^{(1)}_{1,2}\Big| \ge \frac{\delta\kappa_1\kappa_2}{2(L-1)} \;\text{ or }\; \Big|\boldsymbol{V}^{(2)}_{1,2}\Big| \ge \frac{\delta\kappa_1\kappa_2}{2(L-1)}\Big) \\ & \le 2\max\Big\{\; \Pr\Big(\boldsymbol{V}^{(1)}_{1,2} \ge \frac{\delta\kappa_1\kappa_2}{2(L-1)}\Big), \Pr\Big(\boldsymbol{V}^{(2)}_{1,2} \ge \frac{\delta\kappa_1\kappa_2}{2(L-1)}\Big)\;\Big\} \\ & \le 4\exp\Big(-\frac{\delta^2\kappa_1^2\kappa_2^2}{4(N_T-L+1)(L-1)^2\kappa^4}\Big). \end{aligned} \tag{32}$$

These steps can be conveniently extended to the other off-diagonal elements of $\boldsymbol{V}$. According to Gersgorin circle theorem, the eigenvalues of $\boldsymbol{V}$ all lie in L discs. The i-th disc is centering at $\boldsymbol{V}_{i,i}$ with the radius to be

$$r_{i,i} = \sum_{j=1, j\ne i}^{L} |\boldsymbol{V}_{i,j}|. \tag{33}$$

It can be obtained from (32) that

$$\Pr\;(r_{i,i} \ge \delta) \le \Big[4\exp\Big(-\frac{\delta^2\kappa_1^2\kappa_2^2}{4(N_T-L+1)(L-1)^2\kappa^4}\Big)\Big]^{L-1} \tag{34}$$

which is the probability of the event that the eigenvalues of $\boldsymbol{V}$ lie outside $[1-\delta, 1+\delta]$. Based on (17), we show that $\boldsymbol{X}$ satisfies RIP with the probability greater than

$$1 - \Big[4\exp\Big(-\frac{\delta^2\kappa_1^2\kappa_2^2}{4(N_T-L+1)(L-1)^2\kappa^4}\Big)\Big]^{L-1}. \tag{35}$$

IV. Simulation results

The OFDM parameters used in our simulation are set according to [1], as listed in Table I. The bandwidth $B = 12$kHz is centered at $f_c = 27$kHz and divided into $N_c = 512$ OFDM subcarriers, among which $N_p = 70$ and $N_u = 59$ are used for pilot subcarriers and null subcarriers, respectively. The useful length of each OFDM symbol is $T_u = 42.67$ms which equals the reciprocal of the subcarrier spacing. The length of the ZP guard interval is $T_g = \tau_{\max} = 25$ms or equivalently $N_g = 300$ after sampling. Then the length of each OFDM symbol is $T_s = T_u + T_g = 67.67$ms.

We consider the UWA transmission in the unit of OFDM packet which consists of one preamble, one postamble and 64 OFDM symbols, as shown in Figure 2. Both the preamble and

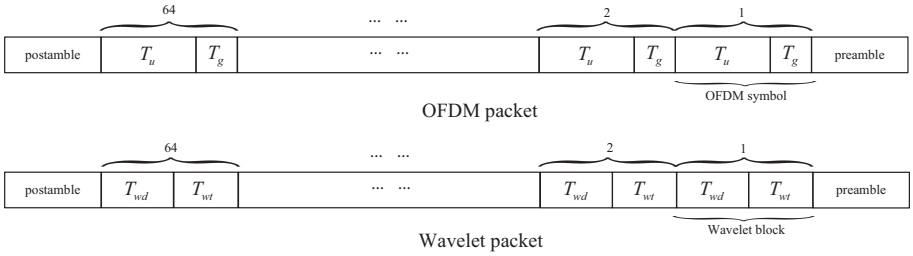

Fig. 2. The structure of OFDM packet and wavelet packet.

TABLE I
PARAMETERS OF OFDM-BASED SYSTEM.

Number of total subcarriers	$N_c = 512$
Number of pilot subcarriers	$N_p = 70$
Number of null subcarriers	$N_u = 59$
Length of zero padding	$N_g = 300$
Carrier frequency	$f_c = 27$kHz
Signal bandwidth	$B = 12$kHz
Doppler shift at f_c	76.98Hz

the postamble are designed to be LFM signals, which are used to mitigate the Doppler effect. Therefore the Doppler scaling factor is regarded as the same within each OFDM packet. The relative speed between the transmitter and the receiver is 8.3 knots, resulting in the Doppler shift at f_c to be around 76.98Hz.

The multipath sparse channel model defined in (1) is used to generate UWA channel data. Within the OFDM packet, a different CIR vector is randomly generate for each OFDM symbol, according to the approach proposed in [7]. $\{\xi_i\}\sim\mathcal{CN}(\mathbf{0}, e^{-b\tau_i}\boldsymbol{I}_S)$. $b = 1/16$ is the exponential power delay profile and τ_i is the delay spread for the i-th path. Here we consider a five-path channel with the maximal channel delay spread $\tau_{\max} = 25$ms. A zero CIR vector with the length L is first generated, where $S = 5$ positions are randomly selected as channel taps. Then we produce $\{\xi_i\}$ as the attenuation for each path. In practice, we may replace the above simulated channel data with the real UWA channel measurements and it's verified in [8] that the simulations usually give the same performance trend as the real UWA experiments.

TABLE II
PARAMETERS OF WAVELET-BASED SYSTEM.

Number of branches in filter bank	$M = 7$
Length of each wavelet symbol	$N_T = 64$
Length of the training symbol	$N_{wt} = 214$
Length of the data symbols	$N_{wd} = 192$
Carrier frequency	$f_c = 27$kHz
Signal bandwidth	$B = 12$kHz
Doppler shift at f_c	76.98Hz

In order to fairly compare the channel estimation performance of OFDM-based and wavelet-based UWA communication systems, we set the length of wavelet packet the same as that of OFDM packet, as shown in Figure 2. The same preamble and postamble are employed. The parameters of the wavelet-based system are listed in Table II. The number of branches is supposed to be $M = 7$ and therefore the length of each wavelet symbol is $N_T = 2^{M-1} = 64$ or equivalently $T_{ws} = 2N_T/B = 10.66$ms. Since the number of total channel taps is $L_w = B\tau_{\max}/2 = 150$, the training length $T_{wt} = 35.67$ms or equivalently $N_{wt} = 214$ is enough to make accurate channel estimation. Then the full data length T_{wd} of each wavelet block is $T_{wd} = T_s - T_{wt} = 32$ms or equivalently $N_{wd} = 192$. We can figure out the number of wavelet data symbols in each wavelet block as $N_{ws} = \lfloor T_{wd}/T_{ws} \rfloor = 3$. The data rate for OFDM-based and wavelet-based system is the same to be $R_o = R_w = 5.67 \times 10^3$ symbols per second (sps). Therefore, we compare two systems under the same conditions of bandwidth, duration, channel profile and data rate. The comparisons of the channel estimation performance in terms of MSE are illustrated in Figure 3. It is observed that the MSE performance of wavelet-based system is better than that of OFDM-based system, especially for large SNR, i.e., SNR> 20dB. For the specific system, we also compare three different CS algorithms, including OMP, StOMP that is an enhanced version of OMP [14], and Homotopy proposed in [7]. In both systems, it's demonstrated that Homotopy outperforms StOMP and OMP.

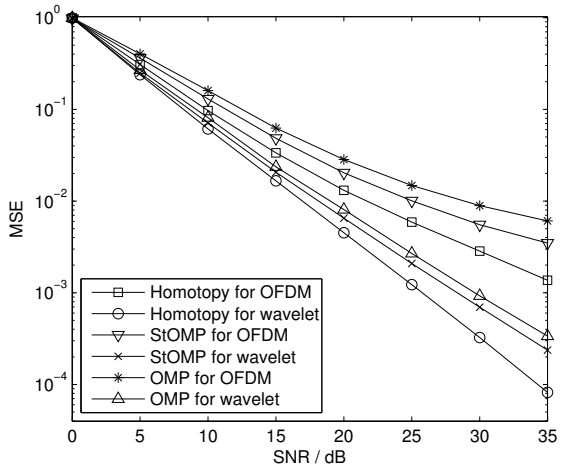

Fig. 3. Comparisons of channel estimation for OFDM-based and wavelet-based UWA communication system ($S = 5$).

Additionally, we also change the number of channel multipath to be $S = 20$ which treats the abundant multipath propa-

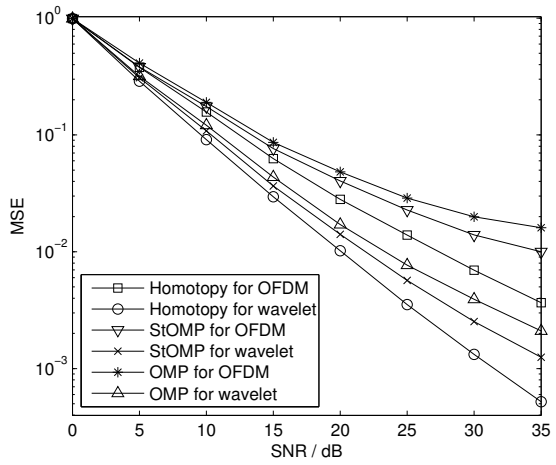

Fig. 4. Comparisons of channel estimation for OFDM-based and wavelet-based UWA communication system ($S = 20$).

gations in UWA channel. The other parameters keep the same. As shown in Figure 4, the performance of channel estimation for $S = 20$ is worse than that of $S = 5$, which implies that the sparser signals are much easier for the recovery. Wavelet-based system still outperforms OFDM-based system.

TABLE III
RUNNING TIMES OF DIFFERENT CS ALGORITHMS.

Algorithm type	CPU time (in seconds)	
	OFDM-based system	Wavelet-based system
Homotopy	0.876	0.584
StOMP	1.211	0.983
OMP	0.849	0.539

The complexities of the OMP, StOMP and Homotopy algorithm for two systems in terms of the CPU running time are compared in Table III where SNR is fixed to be 30dB and $S = 20$. The experiments are performed using MATLAB v7.9 (R2009b) running on a Lenovo laptop with an Intel Core 2 Duo CPU at 2.5GHz and 2GB of memory. We notice that the running time of StOMP is much larger than that of OMP and Homotopy; while the Homotopy is similar to that of OMP. Moreover, the speed of sparse recovery for wavelet-based system is much faster than OFDM-based system. The reason lies in the different size of the measurement matrix in two systems, which directly determines the searching time of two algorithms. In OFDM-based system, we use $N_p = 70$ pilots to reconstruct the sparse UWA channel where $S = 20$ channel taps of totally $N_g = 300$ taps are nonzero and the size of the measurement matrix is 70 by 300. In wavelet-based system, we use $N_{wt} - L_\omega + 1 = 65$ training symbols to reconstruct the UWA channel where $S = 20$ of only $L_w = 150$ channel taps are nonzero. The size of the measure matrix is only 65 by 150, which is much slimmer than that of OFDM-based system.

V. CONCLUSION

In this paper we have proposed a wavelet-based UWA communication system. We have exploited the convolutional structure and formulated the pilot assisted UWA channel estimation as a sparse recovery problem. We have investigated the restricted isometry property (RIP) of the measurement matrix via eigenvalue analysis and Gersgorin circle theorem and proved it satisfies RIP. Simulation results show that the wavelet-based UWA communication systems achieves more accurate UWA channel estimation performance than OFDM-based couterpart under the same conditions of bandwidth, duration, data rate and channel profile.

ACKNOWLEDGEMENTS

The work is supported by the National Natural Science Foundation of China (NSFC) under the Grant 61271204, the Ph.D. Programs Foundation of Ministry of Education of China under the Grant 20120092120014, the National Science and Technology Major Project of China under the Grant 2012ZX03001036-004, the Scientific Research Foundation of Southeast University under the Grant Seucx201116 and Huawei Innovative Research Plan.

REFERENCES

[1] B. Li, S. Zhou, M. Stojanovic, L. Freitag, and P. Willett, "Multicarrier communication over underwater acoustic channels with nonuniform Doppler shifts," *IEEE J. Ocean. Eng.*, vol. 33, no. 2, pp. 198–209, Apr. 2008.

[2] C. R. Berger, Z. Wang, J. Huang, and S. Zhou, "Application of compressive sensing to sparse channel estimation," *IEEE Comm. Mag.*, vol. 48, no. 11, pp. 164–174, Nov. 2010.

[3] H. Ou, J. Allen, and V. Syrmos, "Frame-Based Time-Scale Filters for Underwater Acoustic Noise Reduction," *IEEE J. Ocean. Eng.*, vol. 36, no. 2, pp. 285–297, Apr. 2011.

[4] V. Lottici, R. Reggiannini, and M. Carta, "Pilot-Aided Carrier Frequency Estimation for Filter-Bank Multicarrier Wireless Communications on Doubly-Selective Channels," *IEEE Trans. Sig. Proc.*, vol. 58, no. 5, pp. 2783–2794, May 2010.

[5] S. Baig and H. J. Mughal, "Multirate signal processing techniques for high-speed communication over power lines," *IEEE Comm. Mag.*, vol. 47, no. 1, pp. 70–76, Jan. 2009.

[6] K. Hirakawa and P. Wolfe, "Rewiring Filterbanks for Local Fourier Analysis: Theory and Practice," *IEEE Trans. Inf. Theory*, vol. 57, no. 8, pp. 5360–5374, Aug. 2011.

[7] C. Qi, X. Wang, and L. Wu, "Underwater Acoustic Channel Estimation based on Sparse Recovery Algorithms," *IET Sig. Proc.*, vol. 5, no. 8, pp. 739–747, Dec. 2011.

[8] C. R. Berger, S. Zhou, J. C. Preisig, and P. Willett, "Sparse channel estimation for multicarrier underwater acoustic communication: From subspace methods to compressed sensing," *IEEE Trans. Sig. Proc.*, vol. 58, no. 3, pp. 1708–1721, Mar. 2010.

[9] N. F. Josso, J. J. Zhang, D. Fertonani, A. Papandreou-Suppappola, and T. M. Duman, "Time-varying wideband underwater acoustic channel estimation for OFDM communications," in *Proc. ICASSP*, Dallas, Texas, USA, Mar. 2010, pp. 5226–5629.

[10] S. F. Mason, C. R. Berger, S. Zhou, and P. Willett, "Detection, synchronization, and Doppler scale estimation with multicarrier waveforms in underwater acoustic communication," *IEEE J. Select. Area Commun.*, vol. 26, no. 9, pp. 1638–1649, Dec. 2008.

[11] T. Bianchi, F. Argenti, and E. Re, "Performance of Filterbank and Wavelet Transceivers in the Presence of Carrier Frequency Offset," *IEEE Trans. Comm.*, vol. 53, no. 8, pp. 1323–1332, Aug. 2005.

[12] E. J. Candes and T. Tao, "Decoding by linear programming," *IEEE Trans. Inf. Theory*, vol. 51, no. 12, pp. 4203–4215, Dec. 2005.

[13] G. R. J. Haupt, W. U. Bajwa and R. Nowak, "Toeplitz compressed sensing matrices with applications to sparse channel estimation," *IEEE Trans. Inf. Theory*, vol. 56, no. 11, pp. 5862–5875, Nov. 2010.

[14] D. L. Donoho, Y. Tsaig, I. Drori, and J.-C. Starck, "Sparse solution of underdetermined linear equations by stagewise orthogonal matching pursuit," *Preprint*, 2006.